



ORIGINAL ARTICLE

Polyethylene glycol derivative 9bw suppresses growth of neuroblastoma cells by inhibiting oxidative phosphorylation

Eri Nagasaki-Maeoka¹ | Kazuhiro Ikeda² | Ken-ichi Takayama³ | Takayuki Hirano¹ | Yoshiaki Ishizuka¹ | Tsugumichi Koshinaga¹ | Naoya Tsukune⁴ | Tadateru Takayama⁵ | Satoshi Inoue^{2,3}  | Kyoko Fujiwara^{5,6} 

¹Department of Pediatric Surgery, Nihon University School of Medicine, Itabashi, Japan

²Division of Gene Regulation and Signal Transduction, Research Center for Genomic Medicine, Saitama Medical University, Hidaka, Japan

³Department of Systems Aging Science and Medicine, Tokyo Metropolitan Institute of Gerontology, Itabashi-ku, Japan

⁴Department of Periodontology, Nihon University School of Dentistry, Chiyoda, Japan

⁵Division of General Medicine, Department of Medicine, Nihon University School of Medicine, Itabashi, Japan

⁶Department of Anatomy, Nihon University School of Dentistry, Chiyoda, Japan

Correspondence

Kyoko Fujiwara, Division of General Medicine, Department of Medicine, Nihon University School of Medicine, 30-1 Oyaguchi-Kamicho, Itabashi, Tokyo 173-8610, Japan.
Email: fujiwara.kyoko@nihon-u.ac.jp

Funding information

JSPS Kakenhi, Grant/Award Number: 18K07275 and 19K24131

Abstract

Neuroblastoma (NB) is a childhood malignancy originating from the sympathetic nervous system, and accounts for approximately 15% of all pediatric cancer-related deaths. As the 5-y survival rate of patients with high-risk NB is <50%, novel therapeutic strategies for NB patients are urgently required. Nonaethylene glycol mono(4-iodo-4-biphenyl)ester (9bw) is a polyethylene glycol derivative, synthesized by modifying a compound originally extracted from filamentous bacteria. Although 9bw shows remarkable inhibition of tumor cell growth, the underlying mechanisms remain unclear. Here, we examined the efficacy of 9bw on human NB-derived cells, and investigated the molecular mechanisms underlying the cytotoxic effects of 9bw on these cells. Our results indicated that 9bw induced cell death in NB cells by decreasing the production of ATP. Metabolome analysis and measurement of oxygen consumption indicated that 9bw markedly suppressed oxidative phosphorylation (OXPHOS). Further analyses indicated that 9bw inhibited the activity of mitochondrial respiratory complex I. Moreover, we showed that 9bw inhibited growth of NB in vivo. Based on the results of the present study, 9bw is a good candidate as a novel agent for treatment of NB.

KEYWORDS

anticancer drug, mitochondrial respiratory complex I, neuroblastoma, oxidative phosphorylation, polyethylene glycol derivative

1 | INTRODUCTION

Neuroblastoma (NB) originating from the sympathetic nervous system, including the adrenal medulla and paravertebral nervous trunk, is the most common extracranial solid tumor in childhood.¹ Generally, NB develops in young children, with a median age of 17 mo at diagnosis, and accounts for 15% of all pediatric cancer deaths.¹ NB shows remarkable heterogeneity in biological and clinical features,

with a diverse prognosis. For example, NB with onset at 12 mo old or younger usually shows spontaneous regression or maturation into benign ganglioneuroma. Conversely, most NBs occurring in patients at 18 mo old or older show aggressive phenotypes and poor prognosis.¹ The International Neuroblastoma Risk Group (INRG) classification system divides NB patients into very-low-risk, low-risk, intermediate-risk, and high-risk groups depending on some factors such as age at diagnosis, tumor stage, histology, differentiation grade,

This is an open access article under the terms of the Creative Commons Attribution-NonCommercial-NoDerivs License, which permits use and distribution in any medium, provided the original work is properly cited, the use is non-commercial and no modifications or adaptations are made.

© 2020 The Authors. *Cancer Science* published by John Wiley & Sons Australia, Ltd on behalf of Japanese Cancer Association.

and copy number status at MYCN and chromosome 11q.² Due to the development of multimodal treatment strategies, including surgical resection, multiagent chemotherapy, radiotherapy, autologous hematopoietic stem cell rescue, and immunotherapy, the outcomes of treatments have improved markedly in patients with lower grade NB. However, the 5-y survival rate of patients with high-risk NB is still <50%.³⁻⁵ Therefore, there is an urgent need to develop novel therapeutic strategies for these NB patients with poor outcome.

Nonaethylene glycol mono(4-iodo-4-biphenyl)ester (9bw) is a novel small molecule, with a molecular weight of 675, synthesized as a derivative of a polyethylene glycol compound derived from filamentous bacteria (Figure 1A).⁶ It has been reported previously that 9bw suppressed the growth of tumor cells, such as the mouse abdominal dropsy sarcoma cell line Meth-A and human pancreatic cancer cell line Mia-Paca-2 both in vitro and in vivo.⁶ Peritoneal injection of 9bw suppressed growth of tumors derived from Meth-A and Mia-Paca-2 subcutaneously transplanted in mice without adversely affecting the health of the mice.⁶ These observations suggest that 9bw is a candidate compound for development as a new agent for treatment of NB, however, the mechanisms of action underlying the anticancer effects of 9bw have not been elucidated.

In the present study, we examined the efficacy of 9bw on human NB-derived cells, and investigated the molecular mechanisms underlying the cytotoxic effects of 9bw on these cells. Our data indicated that 9bw induced cell death in NB cells by inhibiting oxidative phosphorylation (OXPHOS). Detailed analyses showed that 9bw inhibits the activity of mitochondrial respiratory complex I, resulting in a decrease of ATP production. Moreover, we showed that 9bw inhibited tumor growth in vivo. The results of the present study strongly suggest that 9bw is a good candidate as a novel agent for treatment of NB.

2 | MATERIALS AND METHODS

2.1 | Cell lines and culture conditions

The human NB-derived cell lines NB9 and SK-N-AS were obtained from the Riken Cell Bank and the American Type Culture Collection (ATCC), respectively. Human dermal fibroblasts (HDF) were obtained from ATCC. NB9 was cultured in RPMI-1640 medium (Nacalai Tesque) supplemented with 10% FBS (Nichirei Bioscience). SK-N-AS and HDF were cultured in DMEM (Nacalai Tesque) supplemented with 10% FBS. All media contained 100 IU/mL penicillin

(Life Technologies) and 100 μ L/mL streptomycin (Life Technologies). Cells were maintained at 37°C in a CO₂ incubator with a controlled humidified atmosphere composed of 95% air and 5% CO₂.

2.2 | Compound

9bw was kindly provided by Mr. Watanabe of Senka Pharmacy Co., Ltd. The compound was dissolved in distilled water to create a 10 mmol/L stock solution and sterilized by filtration. Aliquots were stored at -20°C.

2.3 | Analysis of cell viability

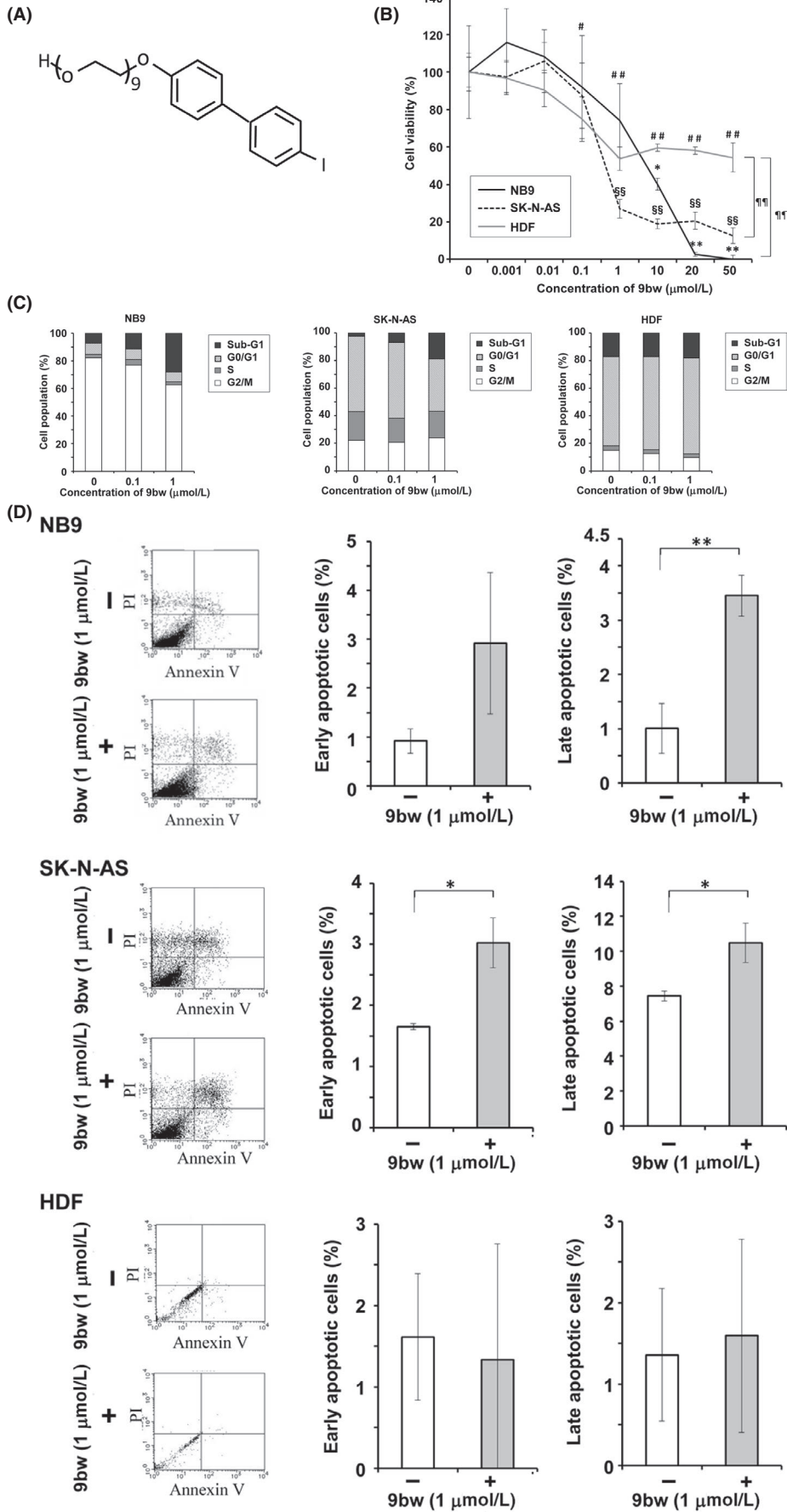
To obtain a dose-response curve for 9bw, NB9 cells, SK-N-AS, and HDF were seeded in 96-well plates at densities of 1×10^4 cells (NB9, HDF) or 2×10^4 cells (SK-N-AS) per well. After 24-h incubation, cells were treated with various concentrations of 9bw for 3 d, and then cell viability was determined by WST8 assay using Cell Count Reagent SF (Nacalai Tesque). For analysis of the efficacy of 9bw under glucose-depleted or glucose-deficient conditions, cells were seeded in 96-well plates at a density of 5×10^4 cells/well. After 24-h incubation, media were replaced with fresh media containing various concentrations of glucose supplemented with or without 1 μ mol/L 9bw. After 72 h of incubation, cell viability was determined by WST8 assay.

2.4 | FACS analysis

For analysis of cell cycle distribution, cells were seeded in culture dishes 100 mm in diameter at a density of 1×10^5 cells (NB9, HDF) or 2×10^5 cells (SK-N-AS) per dish. After 24-h incubation, cells were treated with or without 9bw for 72 h, and then both floating and attached cells were collected. After washing in PBS, cells were fixed in 70% ice-cold ethanol overnight. Subsequently, cells were washed with PBS and incubated in PBS containing 0.1% FBS and 50 μ g/mL of RNase A for 15 min at room temperature, followed by an additional 15-min incubation in the presence of 50 μ g/mL propidium iodide (PI). The stained cells were analyzed for DNA content by flow cytometry (FACSCalibur, BD Biosciences).

The percentage of apoptotic cells was determined using an annexin V-FITC apoptosis detection kit (Bio Vision, Inc) according to the manufacturer's instructions. Briefly, cells were seeded in culture

FIGURE 1 9bw induced cell death of neuroblastoma cells but not normal fibroblasts. A, Chemical structure of 9bw. Cells were treated with various concentrations of 9bw for 3 d, and then (B) cell viability was determined by WST8 assay. Data are shown as means \pm SD. The statistical significance of differences in viability of cells treated with or without 9bw are indicated as follows*, § and # for NB9, SK-N-AS, and HDF, respectively. The statistical significance of differences between HDF and NB cells at 50 μ mol/L 9bw is indicated by ¶, *, §, #, and ¶ indicate $P < .05$; **, §§, ##, and ¶¶ indicate $P < .01$. C, Floating and adherent cells were harvested and fixed with 70% ethanol, followed by staining with propidium iodide (PI) to analyze their cell cycle distributions by FACS. The experiments were performed 3 times, and averages of cell population (%) in each cell cycle phase are shown. D, Floating and adherent cells were harvested and stained with annexin V and PI, and then analyzed by FACS. The experiments were performed 3 times. Representative quadrants and percentages of early apoptotic cells (lower right quadrants) and late apoptotic cells (upper right quadrants) are shown (mean \pm SD). * $P < .05$, ** $P < .01$



dishes 100 mm in diameter at a density of 1×10^5 cells (NB9 and HDF) or 2×10^5 cells (SK-N-AS) per dish and incubated for 24 h. In addition, then media were replaced with fresh media containing various concentrations of glucose supplemented with or without 9bw. After 72 h in culture, both floating and attached cells were collected, and early apoptotic cells (annexin V+/PI-) and late apoptotic cells (annexin V+/PI+) were analyzed by flow cytometry (FACSCalibur; BD Biosciences). The analysis was performed 3 times and the average percentages of apoptotic cells were calculated.

2.5 | Analysis of ATP level in cells

Intracellular ATP level was measured using an ATP assay kit (TOYO-B-Net) in accordance with the manufacturer's instructions. Briefly, cells were seeded in 96-well plates at a density of 5×10^3 cells/well, cultured for 24 h, followed by replacement with new medium containing various concentrations of glucose supplemented with or without 9bw. After 12-h incubation, the intracellular ATP level was measured by monitoring luciferase activity.

2.6 | CE-TOFMS analysis

NB9 cells and SK-N-AS cells were seeded in 10-cm dishes at a density of 2×10^3 cells/dish and 1 $\mu\text{mol/L}$ 9bw was added 24 h after seeding. At 8 h after addition of 9bw, culture medium was removed from the dishes, and cells were washed in 5% mannitol solution. The cells were then treated with methanol and Internal Standard Solution (Human Metabolome Technologies HMT, Inc) to extract intracellular metabolites. After ultrafiltration to remove proteins, metabolic extracts were analyzed using a capillary electrophoresis-time of flight mass spectrometry (CE-TOFMS) system (Agilent Technologies). Peak information, including mass-to-charge ratio (m/z), peak area, and migration time (MT), were determined using automatic integration software (MasterHands, Keio University, Tsuruoka, Japan). The peaks were matched with estimated metabolites from the HMT metabolite library and Known-Unknown peak library based on their m/z values and MTs. The tolerances were set to 10 ppm for m/z and 0.5 min for MT. The concentrations of the metabolites were determined using a standard curve plotted by analyzing standard compounds. For the metabolites without standard compounds, peak areas normalized with internal standards are shown.

2.7 | Analysis of mitochondrial energy metabolism

Oxygen consumption rate (OCR) was measured using a Seahorse Bioscience XFp extracellular flux analyzer (Primetech Corp) in accordance with the manufacturer's instructions. Briefly, cells (5.0×10^3 cells/well) were cultured on XFp plates for 48 h. Prior to the assay, culture medium was replaced by XF Base Medium containing 11.1 mmol/L glucose, 1 mmol/L pyruvate, 2 mmol/L glutamine, adjusted pH to

7.4. Then, 9bw and inhibitors for respiratory complexes, including oligomycin, carbonyl cyanide 4-(trifluoromethoxy)phenylhydrazone (FCCP), and a mixture of rotenone and antimycin A, were loaded into the appropriate ports of a hydrated sensor cartridge. Compounds were sequentially added to the microplates and OCR was monitored.

2.8 | Mitochondrial respiratory complex I activity assay

Mitochondrial respiratory complex I was determined in the presence or absence of 9bw using a MitoCheck Complex I assay kit (catalog no. 700930; Cayman Chemical) according to the manufacturer's instructions. Rotenone was used as a positive control. After mixing all reactants, the absorbance at 340 nm was measured every min for 15 min. Complex I activity was estimated by calculating the decrease in absorbance. All analyses were performed in triplicate.

2.9 | Mitochondrial respiratory complex II/III activity assay

Mitochondrial respiratory complex II/III was determined after addition of 9bw or antimycin as a positive control using MitoCheck Complex II/III assay kit (Cayman Chemicals; catalog no. 700950) according to the manufacturer's instructions. The absorbance of all samples was measured at 550 nm for 15 min using a plate reader. Complex II/III activity was determined by the increase in absorbance per 30 s. All analyses were performed in triplicate.

2.10 | Mitochondrial respiratory complex IV activity assay

Mitochondrial respiratory complex IV was determined after addition of 9bw or KCN as a positive control using a MitoCheck Complex IV assay kit (catalog no. 700990; Cayman Chemicals) according to the manufacturer's instructions. The absorbance of all samples was measured at 550 nm for 15 min using a plate reader. Complex IV activity was determined by the decrease in absorbance per 1 min. All analyses were performed in triplicate.

2.11 | Mouse xenograft model

SK-N-AS cells were suspended in culture medium at a density of 4×10^6 cells/mL, and mixed with an equal amount of Matrigel (BD Biosciences). Aliquots of 100 μL of the mixture containing of 2×10^5 cells were injected using syringes with G27 needles, subcutaneously into the anterior flank of 6-wk-old female NOD-SCID mice. Tumor size was measured using caliper, and tumor volume was calculated using formula $V = \pi/6 \times L \times W \times H$. When the tumor volume reached 100 mm^3 , peritoneal injection of water or 9bw (40 mg/kg body

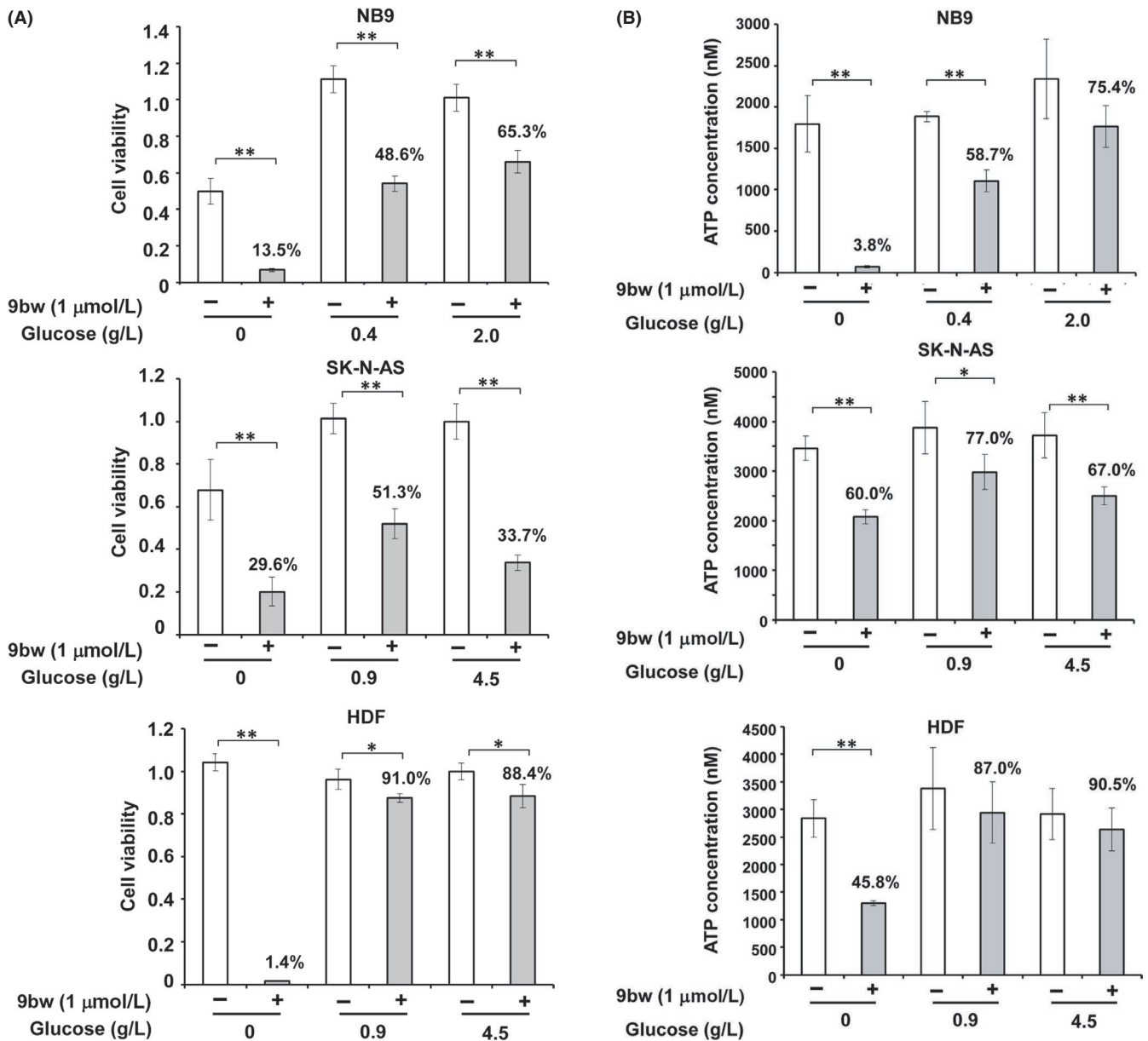


FIGURE 2 9bw strongly induced apoptosis in the absence of glucose. Cells were treated with the indicated concentration of glucose in the presence or absence of 9bw for 3 d. A, Cell viability was determined by WST8 assay. The number over the bar graphs indicates percent cell viability of 9bw treated cells relative to non-treated cells, in each glucose condition. B, ATP levels in the cells were determined by measuring luciferase activity. The number over the bar graphs indicates percent ATP levels in 9bw treated cells relative to non-treated cells, in each glucose condition. Data are shown as means \pm SD. * $P < .05$, ** $P < .01$

weight) was performed and continued twice weekly for 3 wk. Tumor volume and body weight were measured weekly until 3 wk after the first treatment. All experimental procedures performed on animals were approved by the Laboratory Animal Care Committee of Nihon University School of Medicine.

2.12 | Statistical analysis

Statistical analyses were performed using Student *t* test. Data are presented as the mean \pm standard deviation from at least 3 independent experiments. IC_{50} values for 9bw were obtained by using

nonlinear regression curve, calculated using JMP software version 11 (SAS Institute, Inc). In all analyses, a *P*-value $< .05$ was taken to indicate statistical significance.

3 | RESULTS

3.1 | 9bw induced cell death of tumor cells but not normal fibroblasts

To examine the growth inhibitory effect of 9bw, human NB-derived NB9 cells and SK-N-AS cells were treated with various concentrations

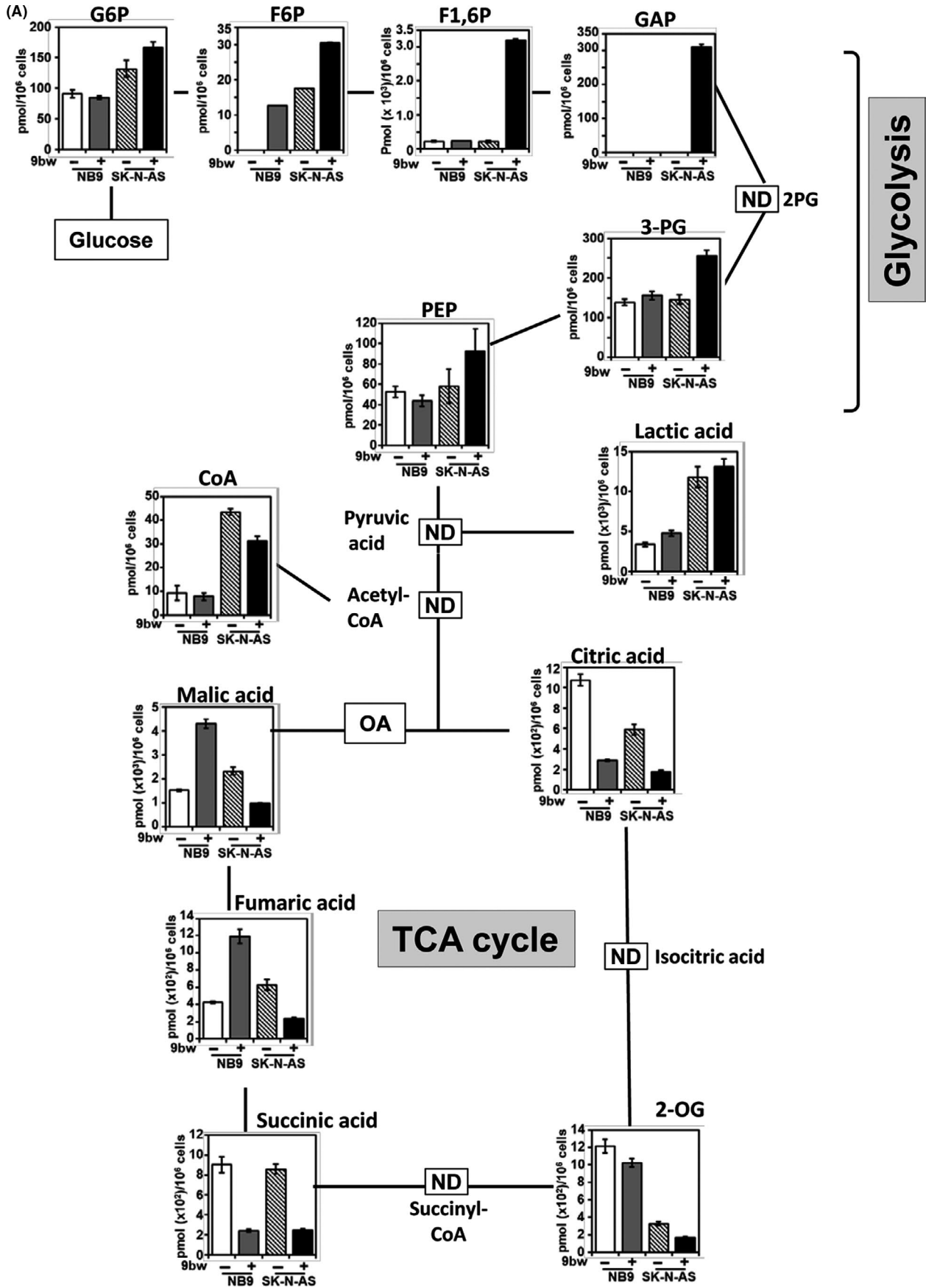


FIGURE 3

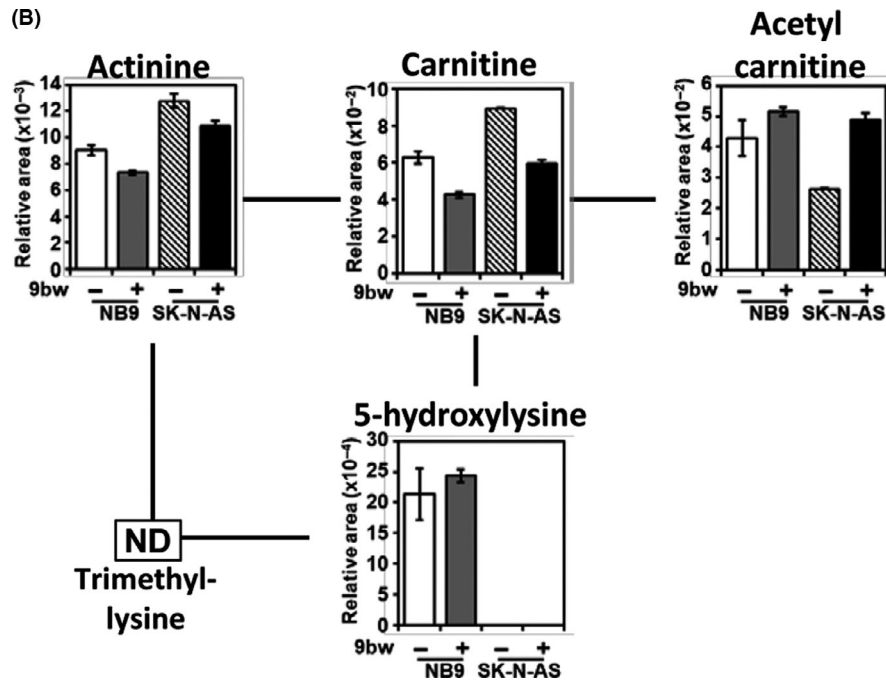


FIGURE 3 Metabolome analysis of extracts of NB9 and SK-N-AS cells treated with or without 9bw. Cells were seeded in 10-cm dishes at a density of 2×10^3 cells/dish, cultured for 24 h, and treated with or without 1 $\mu\text{mol/L}$ 9bw. At 8 h after addition of 9bw, intracellular metabolites were extracted and analyzed by CE-TOFMS. A, Metabolites involved in glycolysis and the TCA cycle, and (B) metabolites of carnitine metabolism. Analyses were performed in triplicate for NB9 and in duplicate for SK-N-AS. Data are shown as means \pm SD. ND, not detected; G6P, glucose-6-phosphate; F6P, fructose-6-phosphate; F1,6P, fructose-1,6-disphosphate; GAP, glyceraldehyde 3-phosphate; 3-PG, 3-phosphoglyceric acid; PEP, phosphoenol pyruvic acid; OA, oxaloacetic acid; 2-OG, 2-oxoglutaric acid

of 9bw for 72 h. As shown in Figure 1B, 9bw suppressed growth of both cell lines in a dose-dependent manner. In NB9, 20 $\mu\text{mol/L}$ or higher amount of 9bw completely suppressed cell growth. In SK-N-AS, 9bw at a concentration ≥ 1 $\mu\text{mol/L}$ suppressed cell viability to as low as ~20%. Conversely, HDF cells treated with 9bw retained cell viability of ~60%, even with treatment at 50 $\mu\text{mol/L}$ 9bw. The IC_{50} values of 9bw for NB9, SK-N-AS, and HDF were 2.52, 0.79 and 38.52 $\mu\text{mol/L}$, respectively.

To clarify how 9bw suppressed the growth of these cells, we examined the possible effects of 9bw on cell cycle distribution. FACS analysis demonstrated that the proportion of cells with sub-G1 DNA content was clearly increased by treatment with 9bw in both NB9 and SK-N-AS cells (Figure 1C). These results indicated that 9bw suppressed cell growth by inducing cell death rather than by inhibiting cell cycle progression. Conversely, HDF did not show an increase in proportion of sub-G1 population in response to 9bw. Instead, the G0/G1 population was slightly increased in 9bw-treated HDF cells. Consistent with these observations, FACS analysis after annexin V/PI staining indicated that the number of apoptotic cells was increased in response to 1 $\mu\text{mol/L}$ 9bw in NB cells but not in HDF (Figure 1D).

3.2 | 9bw reduced ATP level in the cells

During the analyses, we noticed that the culture medium developed a slightly yellow color when cells were cultured for 3 d or longer

in the presence of 9bw. This suggested that glycolysis was accelerated in cells treated with 9bw, resulting in accumulation of lactic acid in the culture medium. To test this hypothesis, we treated the cells with 9bw in culture medium containing no or only a low concentration of glucose for 24 h. As shown in Figure 2A, 9bw suppressed cell viability more strongly under conditions of glucose depletion than in normal medium. Under conditions of glucose depletion, 9bw also markedly reduced the viability of HDF (Figure 2A).

We next analyzed the level of ATP in cells cultured with or without 9bw. Cells were treated with 9bw in culture medium containing different concentrations of glucose for 8 h, followed by measurement of intracellular ATP level. The results clearly indicated that 9bw reduced ATP level in all cells, especially under conditions of glucose depletion (Figure 2B). In SK-N-AS, 9bw significantly reduced ATP level regardless of the concentration of glucose in the culture medium.

3.3 | Cells treated with 9bw showed reduced levels of metabolites involved in the tricarboxylic acid (TCA) cycle

As our data strongly suggested that 9bw affects energy generation and/or energy consumption systems of cells, we profiled the metabolome of cells treated with or without 1 $\mu\text{mol/L}$ 9bw for 8 h to determine

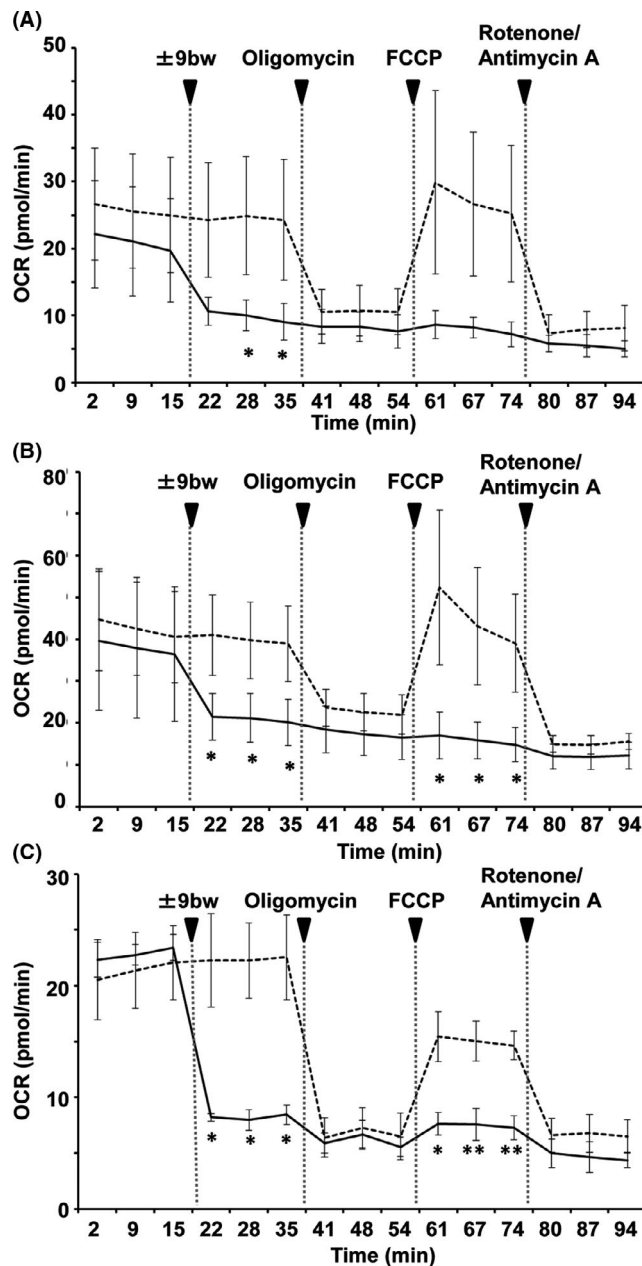


FIGURE 4 Oxygen consumption rate (OCR) of the cells was markedly decreased by treatment with 9bw. Cells were seeded in the culture chamber at a density of 5.0×10^3 cells/well, and cultured for 24 h. 9bw (solid line) or buffer (dashed line), oligomycin, carbonyl cyanide 4-(trifluoromethoxy) phenylhydrazone (FCCP), and rotenone/antimycin A were added to the culture chamber serially, and transitional changes in OCR of the cells were monitored using a Seahorse Bioscience XFp extracellular flux analyzer. A, NB9, (B) SK-N-AS, (C) HDF. Measurements were performed in triplicate. Data are shown as means \pm SD. * $P < .05$, ** $P < .01$

metabolic processes that may be affected by 9bw. Detailed investigation of 219 metabolites that were successfully identified and quantified indicated that the levels of many metabolites involved in the TCA cycle were markedly suppressed in both NB9 and SK-N-AS cells treated with 9bw (Figure 3A). Almost all glycolysis-related metabolites showed increased levels in SK-N-AS, and F6P and lactic acid were increased in

NB9 by treatment with 9bw (Figure 3A). These results indicated that 9bw inhibits ATP generation by the TCA cycle/OXPHOS system, but not by glycolysis. Consistent with this hypothesis, 9bw-treated cells showed decreased levels of carnitine and increased levels of acetyl-carnitine (Figure 3B). As acetyl-carnitine can be formed by the transfer of an acetyl group from acetyl-CoA, which is generated by glycolysis and β -oxidation of fatty acids,^{7,8} reduced carnitine/acetyl-carnitine ratio may also indicate accelerated glycolysis in 9bw-treated cells.

3.4 | 9bw suppressed oxygen consumption rate of cells by inhibiting the activity of mitochondrial respiratory complex I

Next, we examined the effects of 9bw on OCR of the cells. As shown in Figure 4, OCR was suppressed immediately after addition of 9bw in all of SK-N-AS, NB9, and HDF cells. The extent of suppression of OCR by 9bw was almost equivalent to the effects of oligomycin (inhibitor of respiratory complex IV), rotenone (inhibitor of complex I), and antimycin A (inhibitor of complex III). Addition of FCCP, an uncoupler of mitochondrial OXPHOS, did not result in recovery of OCR in the presence of 9bw, suggesting that 9bw inhibited the function of complexes I-IV, but not complex V.

We next examined the effects of 9bw on the activity of mitochondrial respiratory complex I-IV. As shown in Figure 5A, the activity of complex I was significantly reduced in the presence of 1 or 2 μ mol/L 9bw compared to control conditions. Conversely, 9bw did not affect the activity of complex II/III or IV (Figure 5B,C).

3.5 | 9bw suppressed tumor growth in vivo

Finally, we examined the anticancer effects of 9bw in vivo. SK-N-AS cells suspended in Matrigel were injected subcutaneously into each anterior flank region of NOD-SCID mice. When tumor volume reached 100 mm³, 40 mg/kg of 9bw or water was administered intraperitoneally twice a week. Tumor volume was measured at various time points after the first administration. Mice were sacrificed 3 wk after the first injection. Consistent with the results obtained in cultured cells, a marked reduction of tumor volume was observed in 9bw-treated mice compared to controls (Figure 6A). Representative pictures are shown in Figure 6B. There was no difference in body weight between 9bw-treated and control mice (Figure 6C). In addition, close inspection of their viscera, including the liver, kidney, spleen, and lungs, revealed no abnormalities in 9bw-treated animals (data not shown). These results strongly suggested that 9bw possesses tumor-suppressive activity without showing apparent adverse effects on normal organ function in vivo.

4 | DISCUSSION

The results of the present study indicated that a novel polyethylene glycol derivative, 9bw, induced death of NB cells but not normal fibroblasts.

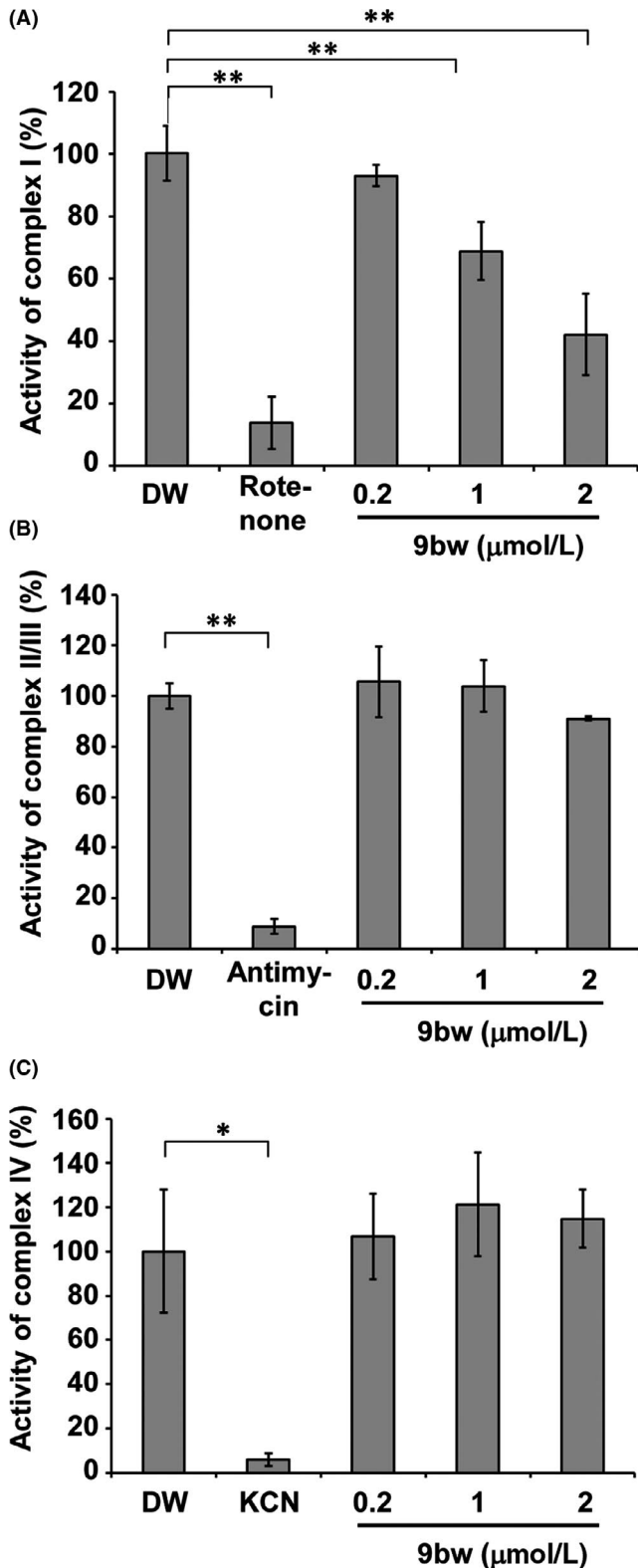


FIGURE 5 9bw suppressed the activity of mitochondrial respiratory chain complex I. A, Activity of mitochondrial respiratory chain complex I was measured using a MitoCheck Complex I assay kit in the presence or absence of 9bw. Rotenone was used as a positive control. B, Activities of mitochondrial respiratory chain complex II and III were measured using a MitoCheck Complex II/III assay kit in the presence or absence of 9bw. Antimycin was used as a positive control. C, The activity of mitochondrial respiratory chain complex IV was measured using a MitoCheck Complex IV assay kit in the presence or absence of 9bw. KCN was used as a positive control. All analyses were performed in triplicate. Data are shown as means \pm SD. * $P < .05$, ** $P < .01$

Although susceptibility to 9bw varied between cells, 9bw decreased OCR to an almost equivalent extent in all cells analyzed. These findings indicated that susceptibility to 9bw may be dependent on the tolerance of the cells to ATP depletion or on the dependence of the cells on OXPHOS for ATP production. The viability of HDF was markedly suppressed only when the medium was completely depleted of glucose. Cell death was hardly induced in HDF cells by 9bw when cultured in medium containing glucose. As 9bw significantly reduced ATP level in HDF only when cells were cultured in glucose-depleted medium, we speculated that HDF showed less dependence on OXPHOS for ATP production than NB cells.

Some OXPHOS inhibitors have been developed as novel therapeutics for cancer.⁹⁻¹² The STAT3 inhibitor, OPB-111077, was reported to show anticancer effects, at least in part through suppression of OXPHOS in cancer cells, because STAT3 promotes tumorigenesis both by regulating expression of protumorigenic genes and by regulating mitochondrial respiratory complex I and II.^{10,13-15} IACS-010759 is an inhibitor of complex I, initially identified through drug screening of HIF-1 α modulators, exhibiting a strong anticancer effect on cell lines derived from brain tumor and acute myeloid leukemia reliant on OXPHOS.¹¹ Gboxin, a small molecule identified by high-throughput screening of specific anticancer drugs for glioblastoma, was demonstrated to suppress growth of glioblastoma in vitro and in vivo by inhibition of complex V.¹² Although these compounds are under investigation for clinical applicability, these findings strongly suggest that OXPHOS is an ideal target for specific and effective cancer therapeutics.

Similar to the above-mentioned OXPHOS inhibitors, 9bw is a small molecule that is easily taken up into cells without the need for a drug carrier, and suppresses OCR of cells immediately after administration, as demonstrated in the present study. Based on these features, 9bw has potential for development as an anticancer drug. Treatment of high-risk neuroblastoma patients has improved over the past several decades, and multiagent chemotherapy and antibodies to disialoganglioside GD2 have improved the prognosis of patients.^{5,16,17} Molecular targeting drugs, such as anaplastic lymphoma kinase (ALK) inhibitors for cases with mutation or amplification of the ALK gene,^{18,19} and drugs that affect MYCN transcription, stability of MYCN, or MYCN-dependent metabolic changes^{5,20-22} are under development. Nevertheless, the

Detailed analyses revealed that 9bw induced cell death by inhibiting ATP production through OXPHOS. OCR of the cells was completely suppressed by 9bw treatment, and further analyses indicated that this was due to inhibition of mitochondrial respiratory complex I (Figure 7). In addition, administration of 9bw significantly suppressed tumor growth in vivo without obvious adverse effects on the health of mice.

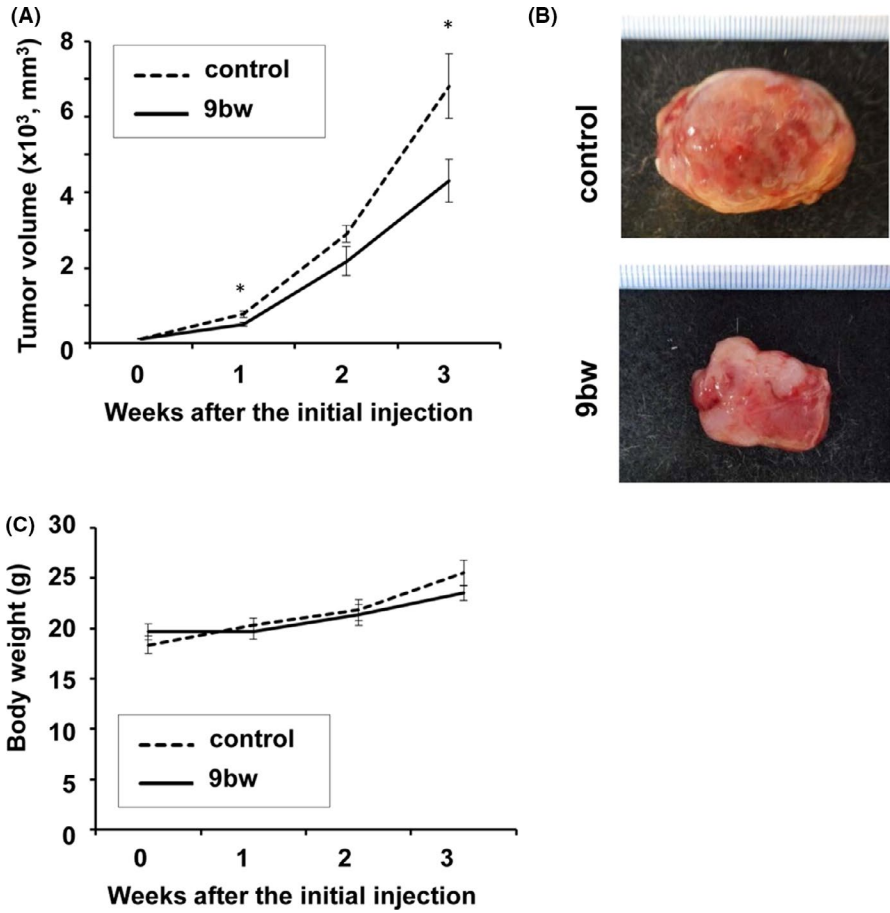


FIGURE 6 9bw suppressed tumor growth in vivo. A, C, SK-N-AS cells were injected subcutaneously into immunodeficient NOD/SCID mice, and 9bw or distilled water was applied intraperitoneally twice a week. Tumor volume and body weight were measured at the indicated time points after the first injection. Data are shown as mean ± SEM. **P* < .05 (B) Representative photographs of tumors at dissection are shown

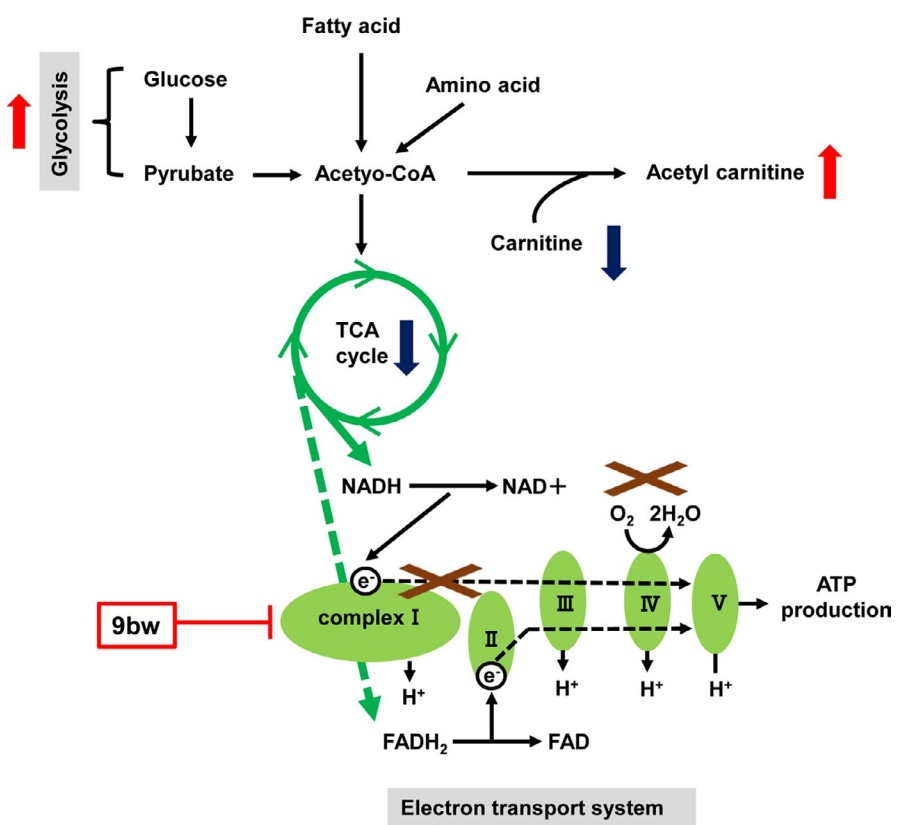


FIGURE 7 Model for 9bw-mediated OXPHOS inhibition. Suppression of OXPHOS by inhibiting mitochondrial respiratory complex I resulted in reduced activity of the TCA cycle and increased activity of glycolysis. The red arrows indicate that the amount of metabolites were increased in 9bw treated cells, and the blue arrows are for decreased metabolites in metabolome analysis. The cross marks indicate the reaction suppressed in the presence of 9bw

5-y survival rate of patients with high-risk NB is still <50%.³⁻⁵ The observation that 9bw induced cell death in both MYCN amplification negative SK-N-AS and positive NB9 suggests that this agent may have anticancer efficacy in high-risk NB. Actually, IC₅₀ of 9bw for MYCN amplification negative cell line SK-N-AS and SK-N-SH were 0.79 and 4.844 μmol/L, for MYCN amplification positive cell line NB1, NB9, and Kelly were 6.871, 2.517 and 3.881 μmol/L (Figures 1 and S1). These data indicate that MYCN amplification status may not affect the efficacy of 9bw.

Taken together, the findings presented here strongly suggest that 9bw has potential for development as a new agent for treatment of NB. As 9bw is novel compound and does not have similarity with other OXPHOS inhibitors, the molecular mechanism underlying the suppression of OCR by 9bw remains unclear. Further studies to determine how 9bw suppresses the activity of mitochondrial respiratory complex I are currently ongoing in our laboratory.

ACKNOWLEDGMENTS

We thank Ms A. Oguni for her excellent technical assistance and Ms K. Tagata for her secretarial assistance. We are grateful to Mr. Hisanori Watanabe in Senca Pharmacy Co. Ltd. for supplying 9bw. This work was supported by JSPS KAKENHI Grant Number 18K07275 to KF and 19K24131 to NT

DISCLOSURE

The authors declare no conflicts of interest.

ORCID

Satoshi Inoue  <https://orcid.org/0000-0003-1247-3844>

Kyoko Fujiwara  <https://orcid.org/0000-0002-1751-7968>

REFERENCES

- Maris JM, Hogarty MD, Bagatell R, Cohn SL. Neuroblastoma. *Lancet*. 2007;369(9579):2106-2120.
- Bosse KR, Maris JM. Advances in the translational genomics of neuroblastoma: from improving risk stratification and revealing novel biology to identifying actionable genomic alterations. *Cancer*. 2016;122(1):20-33.
- Maris JM. Recent advances in neuroblastoma. *N Engl J Med*. 2010;362(23):2202.
- Park JR, Bagatell R, London WB, et al. Children's Oncology Group's 2013 blueprint for research: neuroblastoma. *Pediatr Blood Cancer*. 2013;60(6):985-993.
- Irwin MS, Park JR. Neuroblastoma: paradigm for precision medicine. *Pediatr Clin North Am*. 2015;62(1):225-256.
- Senca Pharmacy Co., Ltd. Polyethylene glycol derivatives and anticancer drugs containing them. JP5364532B2. 2013-12-11.
- Ramsay RR, Zammit VA. Carnitine acyltransferases and their influence on CoA pools in health and disease. *Mol Aspects Med*. 2004;25(5-6):475-493.
- Altamimi TR, Thomas PD, Darwesh AM, et al. Cytosolic carnitine acetyltransferase as a source of cytosolic acetyl-CoA: a possible mechanism for regulation of cardiac energy metabolism. *Biochem J*. 2018;475(5):959-976.
- Cheong JH, Park ES, Liang J, et al. Dual inhibition of tumor energy pathway by 2-deoxyglucose and metformin is effective against a broad spectrum of preclinical cancer models. *Mol Cancer Ther*. 2011;10(12):2350-2362.
- Tolcher A, Flaherty K, Shapiro GI, et al. A first-in-human phase I study of OPB-111077, a small-molecule STAT3 and oxidative phosphorylation inhibitor, patients with advanced cancers. *Oncologist*. 2018;23(6):658.e72.
- Molina JR, Sun Y, Protopopova M, et al. An inhibitor of oxidative phosphorylation exploits cancer vulnerability. *Nat Med*. 2018;24(7):1036-1046.
- Shi Y, Lim SK, Liang Q, et al. Gboxin is an oxidative phosphorylation inhibitor that targets glioblastoma. *Nature*. 2019;567(7748):341-346.
- Meier JA, Larner AC. Toward a new STATe: the role of STATs in mitochondrial function. *Semin Immunol*. 2014;26(1):20-28.
- Wegrzyn J, Potla R, Chwae YJ, et al. Function of mitochondrial Stat3 in cellular respiration. *Science*. 2009;323(5915):793-797.
- Genini D, Brambilla L, Laurini E, et al. Mitochondrial dysfunction induced by a SH2 domain-Targeting STAT3 inhibitor leads to metabolic synthetic lethality in cancer cells. *Proc Natl Acad Sci USA*. 2017;114(25):E4924-E4933.
- Pearson AD, Pinkerton CR, Lewis IJ, Imeson J, Ellershaw C, Machin D. High-dose rapid and standard induction chemotherapy for patients aged over 1 year with stage 4 neuroblastoma: a randomised trial. *Lancet Oncol*. 2008;9(3):247-256.
- Yu AL, Gilman AL, Ozkaynak MF, et al. Anti-GD2 antibody with GM-CSF, interleukin-2, and isotretinoin for neuroblastoma. *N Engl J Med*. 2010;363(14):1324-1334.
- Siaw JT, Wan H, Pfeifer K, et al. Brigatinib, an anaplastic lymphoma kinase inhibitor, abrogates activity and growth in ALK-positive neuroblastoma cells, Drosophila and mice. *Oncotarget*. 2016;7(20):29011-29022.
- Wang Y, Wang L, Guan S, et al. Novel ALK inhibitor AZD3463 inhibits neuroblastoma growth by overcoming crizotinib resistance and inducing apoptosis. *Sci Rep*. 2016;6:19423.
- Puissant A, Frumm SM, Alexe G, et al. Targeting MYCN in neuroblastoma by BET bromodomain inhibition. *Cancer Discov*. 2013;3(3):309-323.
- Barone G, Anderson J, Pearson ADJ, Petrie K, Chesler L. New strategies in neuroblastoma: therapeutic targeting of MYCN and ALK. *Clin Cancer Res*. 2013;19(21):5814-5821.
- Hogarty MD, Norris MD, Davis K, et al. ODC1 is a critical determinant of MYCN oncogenesis and a therapeutic target in neuroblastoma. *Cancer Res*. 2008;68(23):9735-9745.

SUPPORTING INFORMATION

Additional supporting information may be found online in the Supporting Information section.

How to cite this article: Nagasaki-Maeoka E, Ikeda K, Takayama K-I, et al. Polyethylene glycol derivative 9bw suppresses growth of neuroblastoma cells by inhibiting oxidative phosphorylation. *Cancer Sci*. 2020;111:2943-2953. <https://doi.org/10.1111/cas.14512>